Superfluid density of ^{3}He in 98% aerogel in small magnetic fields

E. Nazaretski,[1,2] D. M. Lee,[1] and J. M. Parpia[1]
[1]*Laboratory of Atomic and Solid State Physics, Cornell University, Ithaca, New York 14853, USA*
[2]*Los Alamos National Laboratory, Los Alamos, New Mexico 87545, USA*
(Received 12 October 2004; published 15 April 2005)

We performed low-frequency sound measurements on ^{3}He in 98% aerogel in a magnetic field that was varied between 0 and 2130 G at a fixed pressure of 27.9 bar. We monitor the frequency of the second sound like (slow) mode, which is the manifestation of superfluidity of ^{3}He in the presence of correlated disorder, and use its temperature dependence to calculate the superfluid fraction ρ_s/ρ. We observed no field dependence of the $\rho_s(T)/\rho$, other than an increase in the temperature range where the *A*-like (A^*) phase is metastable. Both the A^* and *B* phases have a smaller $\rho_s(T)/\rho$ than that of bulk ^{3}He, and the ratio $\rho_s^{A^*}/\rho_s^B$ is $\approx$0.5 over the whole temperature range. The A^* phase does not reappear on warming from the *B* phase until a field in excess of 1270 Gauss is applied.

DOI: 10.1103/PhysRevB.71.144506 PACS number(s): 67.57.De, 67.57.Pq, 68.05.−n, 68.18.Jk

I. INTRODUCTION

^{3}He is recognized as an extremely pure system that undergoes a transition from a normal Fermi-liquid to a *p*-wave superfluid at low enough temperatures. It has been found that a very dilute network of silica strands, aerogel, acts as an impurity in ^{3}He.[1] Typical aerogels used in ^{3}He studies have a porosity of $\sim$98% (Refs. 2–5) and exhibit fractal structure with a distribution of correlation lengths between a few nanometers and 100 nm. Since the silica particles' diameter ($\sim$2–5 nm) is smaller than the superfluid ^{3}He coherence length (ξ_0=15–80 nm), aerogel acts as a collection of correlated impurities enabling the study of disorder on a strongly interacting Fermi liquid. The aerogel has a significant effect on the ^{3}He phase diagram, which exhibits different features compared to bulk ^{3}He. The most obvious is the suppression of the superfluid transition T_c and of the superfluid density ρ_s/ρ.[1,6] In addition the *A*-like phase appears to be highly hysteretic, displaying an enhanced supercooling,[7–9] together with stable coexistence of the *A*-like and *B* phases[7,9–11] observed under specific preparation conditions. Further, on warming in zero field, the *A* like phase fails to reappear except perhaps in a region of width $\leqslant$20 μK below the superfluid transition, T_{ca}.

In the work reported here, we used the low-frequency sound technique to obtain the superfluid density, ρ_s/ρ of ^{3}He confined to 98% aerogel in a magnetic field. The measurements carried out in both the isotropic *B* phase and the metastable *A*-like phase (which we refer to as the A^* phase throughout the paper) reveal that the superfluid component of the A^* phase $\rho_s^{A^*}$, which we had found to be suppressed to $\approx$0.5 ρ_s^B in zero field, continues to be suppressed by the same factor in fields up to 1270 G. The $B\rightarrow A^*$ transition was not seen in ρ_s/ρ on warming until a field $>$1270 G was applied, calling into question whether the A^* phase is really the lowest energy (equilibrium) phase in low fields at this pressure. Alternatively, the *B* phase must exhibit superheating (unlike the bulk) and persist to near T_{ca} in a metastable state.

Although several measurements using various experimental techniques have been performed in the ^{3}He-98% open aerogel system, the question of whether A^* phase is actually the bulk *A* phase or a different equal-spin-paired state is still unanswered.[12,13] Experiments in a 99.3% open aerogel (that is significantly more open) identify the A^* phase as the Planar state.[14] Most theoretical investigations[15–17] have concentrated on the *B* phase, which has been conclusively identified through NMR.[11,18,19]. Hänninen *et al.*[20] and Higashitani *et al.*[21] calculate the suppression factors for the two components of the anisotropic *A* phase and for the *B* phase. These theoretical results will be compared to experimental behavior that shows $\rho_s^{A^*}/\rho_s^B \approx 0.5$.[22] More recent work has elucidated the role of the solid ^{3}He layer in the suppression of the high-field A_1 phase.[23] With the question of the existence of the A_1 phase now settled,[24] attention should turn to the nature of the A^* phase. In bulk and conventionally confined ^{3}He, other possible phases were proposed[25–27] but not experimentally observed.

II. EXPERIMENTAL METHOD

Two-fluid hydrodynamics describes a superfluid as a combination of two interpenetrating normal and superfluid components.[28] In the presence of an elastic matrix (aerogel), the normal fluid component is clamped to the matrix, since the viscous penetration depth exceeds the characteristic separation of the silica strands in aerogel and can oscillate either in phase or out of phase with the superfluid component, giving rise to the so-called fast and slow modes, which are equivalent to a compressional wave and second sound in bulk, respectively. The slow mode also corresponds to fourth sound in rigid porous media. McKenna *et al.* observed the second sound like mode in ^{4}He in aerogel,[29] modified the conventional two-fluid hydrodynamic equations by coupling the normal component to the elastic skeleton of aerogel, and showed that the antisymmetric (slow) and symmetric (fast) modes could propagate in the superfluid. Analysis of the slow-mode velocity as a function of temperature provides information about the superfluid fraction in the ^{3}He-aerogel system and can be described by the following equation:

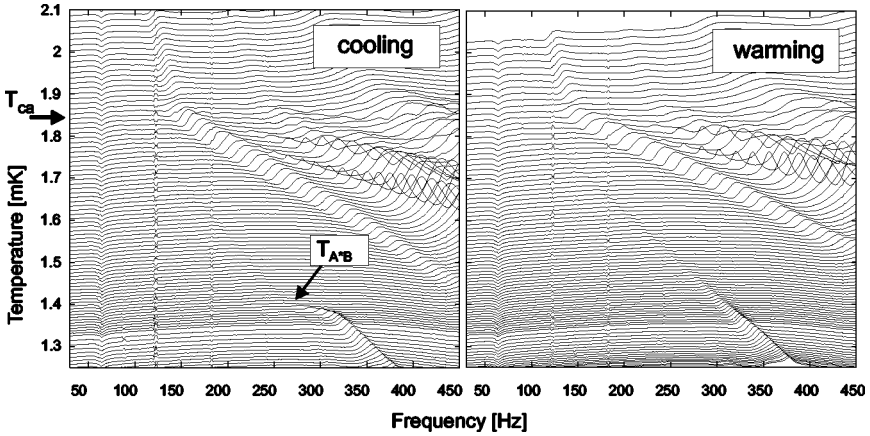

FIG. 1. Examples of the slow mode observed for superfluid ^{3}He in 98% aerogel. Data were taken at pressure $P=27.9$ bar and $B=747$ G. The left panel shows the evolution of the slow mode on cooling and the right panel on warming. Only 20% of the data are shown for clarity. The y axis has an offset with temperature. The weaker low-frequency mode seen both on cooling and warming is the fundamental second sound like mode that appears at $T_{ca}=1.85$ mK. Above T_{ca} it transforms into the "edge mode" (see text for details). The sharp kink on cooling at $\sim$1.35 mK signals the onset of the $A^*\rightarrow B$ transition. No $B\rightarrow A^*$ transition was observed on warming at $B=747$ G. The stronger modes at higher frequencies are attributed to the resonances arising from combinations of the Helmholtz mode and harmonics of the slow mode.

$$\frac{\rho_s}{\rho}=\left\{\frac{\rho_a}{\rho}\left[\left(\frac{c_a}{c_s}\right)^2-1\right]+1\right\}^{-1}, \tag{1}$$

which in the limit of $c_s^2 \ll c_a^2$ can be rewritten as

$$\frac{\rho_s}{\rho}=\frac{\rho}{\rho_a}\left(\frac{c_s}{c_a}\right)^2, \tag{2}$$

where c_s is the slow mode velocity and c_a is the longitudinal sound velocity in aerogel. ρ_a and ρ are the densities of aerogel and bulk ^{3}He, respectively.

III. CELL AND MEASURING TECHNIQUE

We studied the low-frequency sound propagation of ^{3}He in aerogel[30] in a pure silver cell (chosen to minimize the specific heat in a magnetic field). The 98% aerogel sample ($\sim$1 cm^3) has a cylindrical shape and was inserted in a close-fitting cavity in the cell body. Two coin silver wafers with 0.5 mm thick piezoceramic $PbTiO_3$ disks glued on top, capped off the cavity at either end and functioned as microphone and speaker. Coin silver was used because of its superior elastic properties (compared to pure silver) and moderate specific heat in the presence of a field. Both transducers were in contact with the aerogel, which ensured that the aerogel was clamped in the cell body. The ^{3}He inside the cell was cooled by a $\sim$3.2 cm^3 silver sinter heat exchanger. The experimental cell was mounted on a nuclear demagnetization cryostat with a copper nuclear stage. A vibrating wire viscometer and ^{3}He melting-curve thermometer monitored the temperature of ^{3}He in the cell and on the experimental plate of the cryostat. To minimize the radiation of the sound field into the heat exchanger and vibrating wire volumes we reduced the diameter of the channels connecting these to the sound cell down to 0.5 mm.

We applied an ac drive to the speaker and used a lock-in amplifier connected to the microphone to detect the response of the ^{3}He-aerogel system. The frequency was swept in the range between 5 and 450 Hz. All measurements were taken at a fixed pressure of 27.9 bar, and we varied the field between 0 and 2130 G.

IV. EXPERIMENTAL RESULTS

An example of the second sound like mode at $B=747$ G is shown in Fig 1. The left and right panels show the evolution of the slow mode on cooling and warming, respectively. The sharp kink at $\sim$1.35 mK is the signature of the $A^*\rightarrow B$ transition that was observed only on cooling in this field. The cooling rate was varied between 10 and 50 μK/h, and the $A^*\rightarrow B$ transition always occurred at the same temperature and displayed a characteristic width of $\sim$20 μK, in accord with the zero field data obtained in the same aerogel sample.[22] Also, we did not observe any history dependence of the $A^*\rightarrow B$ transition. Using Eq. (2) we calculate the superfluid fraction of ^{3}He in aerogel versus temperature. To determine ρ_s/ρ accurately, we had to account for the "edge mode" contribution. The so-called edge mode is associated with the longitudinal oscillations of bulk superfluid ^{3}He in a thin sliver between the aerogel cylinder and the walls of the experimental cell. This edge mode was observed earlier by Golov *et al.*[6] for superfluid ^{3}He in aerogel and by Mulders *et al.*[31] for superfluid ^{4}He in aerogel. Its sound velocity can be expressed as $c_{\rm edge}=\mathrm{A}\cdot(\rho_s^{\rm bulk}/\rho^{\rm bulk})^{1/2}$, where A is a geometry-dependent constant. The bulk ^{3}He-B normal fluid density can be described through the low-temperature form of the Yoshida function, $Y(t)$[32] and in the simplest case the relation between the normal fraction, $\rho_n^{\rm bulk}/\rho^{\rm bulk}$ and temperature can be written as

$$\frac{\rho_n^{\rm bulk}}{\rho^{\rm bulk}}\propto t^{-1/2}e^{-\Delta_B/t}, \tag{3}$$

where $t=T/T_c^{\rm bulk}$ is the reduced temperature and Δ_B is the energy gap. We find that we can fit the edge-mode contribu-

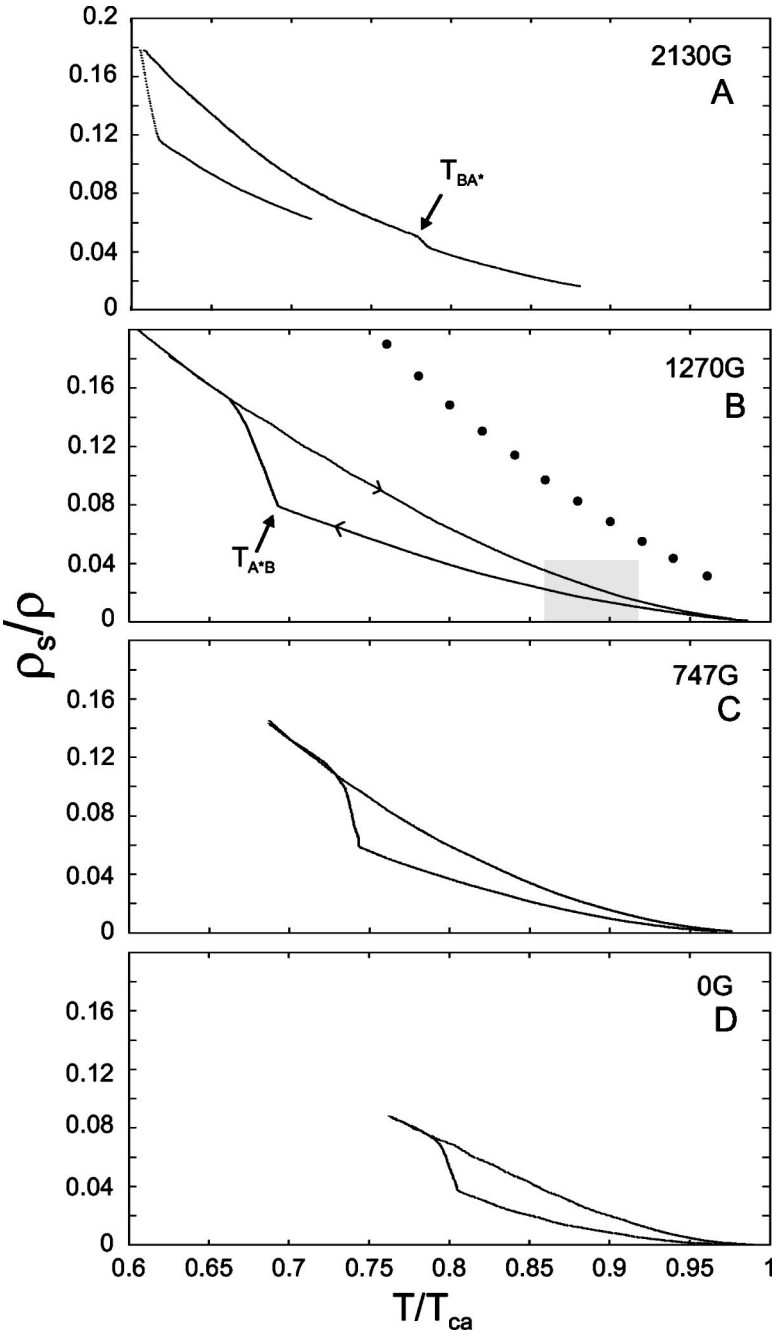

FIG. 2. Superfluid fraction ρ_s/ρ calculated using Eq. (2) on cooling and warming. Experimental parameters: (A) $P=27.9$ bar and $B=2130$ G, (B) $B=1270$ G, and (C) $B=747$ G. For the data obtained in 2130 G, the $A^*\rightarrow B$ transition did not proceed to completion because of limited cooling power. Above T_{A^*B}, the superfluid fraction $\rho_s^{A^*}$ is approximately one-half of the magnitude of ρ_s^B. Once the $A^*\rightarrow B$ transition is completed (in the lower three panels) both the cooling and warming traces are identical. Filled circles in panel (B) show the superfluid fraction in bulk ^{3}He at $P=24.13$ bar[33] to illustrate the difference in the bulk and disordered superfluid fractions. The gray box in this panel marks the region where we expect to see a $B\rightarrow A^*$ transition (see text and Fig. 4). The data in panel (D) were taken from Ref. 22, where ^{3}He in the same aerogel sample was studied in zero field.

tion with an accuracy better than 10% using the parameters $A=5.2$ m/s and the values of $\rho_n^{\mathrm{bulk}}/\rho^{\mathrm{bulk}}$ versus T at $P=29.1$ bar taken from Ref. 33.

Examples of the superfluid fraction, ρ_s/ρ at $B=2130$ G, 1270 G, 747 G, and earlier data in 0 G (after subtraction of the edge-mode contribution) are shown in Fig. 2. In all cases, the lower trace was taken on cooling and the upper one on warming. There is a significant difference in the magnitudes of the ρ_s/ρ of the metastable A^* (seen while cooling) and the B phase, which appears at low temperatures and persists to T_{ca} on warming in Fig. 2(B)–2(D). $\rho_s^{A^*}/\rho_s^B\approx 0.5$, and we discuss this in greater detail later on. Once the $A^*\rightarrow B$ transition is completed, the behavior of the cooling and warming traces is identical. Our experiments showed no field dependence of ρ_s/ρ in the A^* and the B phase. The absolute values of ρ_s/ρ at $P=27.9$ bar were found to be in good agreement with earlier reported zero-field data at a similar pressure.[6,7] In Fig. 2B we also plot the $\rho_s^{\mathrm{bulk}}/\rho$ values (filled circles) measured in the bulk B phase[33] at $P=24.17$ bar to emphasize the suppression of ρ_s/ρ in ^{3}He in aerogel compared to bulk ^{3}He.

Figure 3 is a temperature-frequency plot that shows the evolution of the slow mode's frequency at $B=2130$ G (solid line) as the sample was cooled down and warmed up. The dotted line represents the 747 G data where the $A^*\rightarrow B$ transition occurred only on cooling (i.e., the $B\rightarrow A^*$ transition was not observed on warming). The cooling trace extends the temperature evolution of the slow mode measured at 747 G and shows the suppression of T_{A^*B} in higher fields. At $T=1.1$ mK and $B=2130$ G, the $A^*\rightarrow B$ transition is manifested by a sharp kink. We infer that the $A^*\rightarrow B$ transition did not

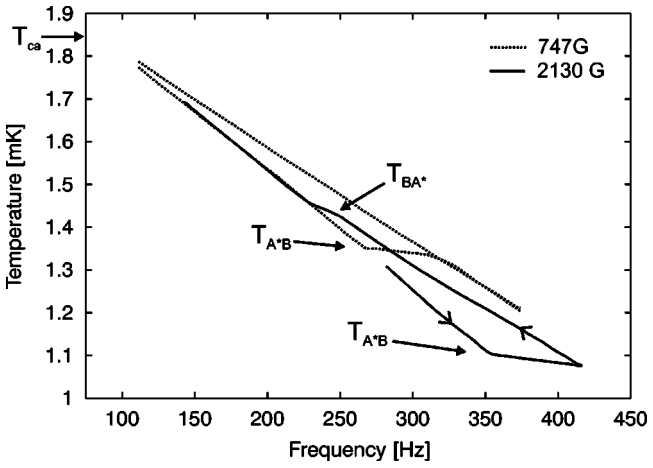

FIG. 3. The slow mode frequency vs temperature. The dotted and solid lines show data in 747 G and 2130 G, respectively. Arrows mark the cooling and warming directions. The temperature of the $A^* \rightarrow B$ transition is significantly suppressed by the magnetic field. At $B=2130$ G the $A^* \rightarrow B$ transition is incomplete. This is inferred from the observation that the warming trace lies to the left of the data points obtained in the B phase (while warming) at $B=747$ G. The $B \rightarrow A^*$ transition is observed at $T=1.45$ mK.

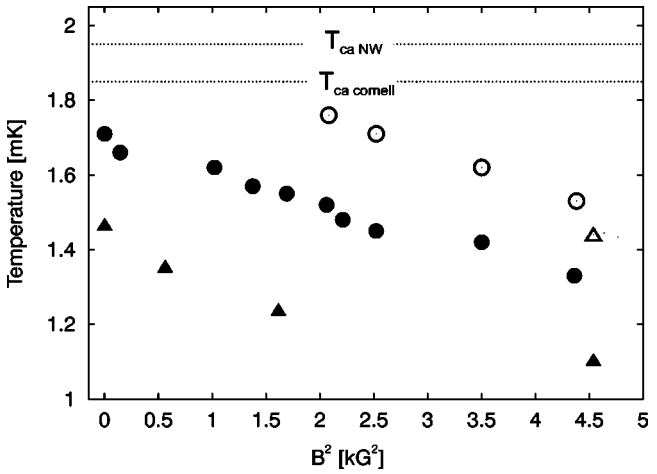

FIG. 4. The temperature of the $A^* \rightarrow B$ and $B \rightarrow A^*$ transition vs magnetic field. (▲) represent our data on cooling demonstrating the effect of supercooling. The zero-field point was taken from earlier experiments on the same sample[7] (△) shows the $B \rightarrow A^*$ transition. Circles show the data obtained at $P=25$ bar using the ultrasound technique by Gervais *et al.*[4] (●) represent the supercooled $A^* \rightarrow B$ transition, and (○) the $B \rightarrow A^*$ transition on warming. The two different values of T_{ca} are indicated by dotted lines.

proceed to completion because the warming trace at 2130 G lies between the cooling and warming traces taken at 747 G. The $B \rightarrow A^*$ transition occurs at $T=1.45$ mK, and once it is complete the slow mode frequency falls on the corresponding A^* cooling trace taken at 747 G. This was the only $B \rightarrow A^*$ transition we observed in our experiments.

The temperature independent stable coexistence of the A^* and B phases seen in the 2130 G data is similar to our earlier observations in zero field.[7,22] Our findings do not agree with the results of Moscow group[11] who used pulsed NMR to measure the relative fraction of the A-like and B phase versus temperature below T_{ca}. They observed a slow conversion from the A-like into the B phase below T_{ca}, with a rate determined by the proximity in temperature to the $A^* \rightarrow B$ transition. At $P=25.5$ bar and $B=284$ G the conversion proceeded over several hours at $T/T_{ca} \approx 0.9$, while it took only several minutes at $T/T_{ca} \approx 0.8$. The discrepancy in the low-frequency sound and NMR results suggest that the magnetic field, which modifies textures in the bulk and the surface solid ^{3}He (whose magnetization may play a role in the stabilities of the A^* and B phases), cannot provide the mechanism for the metastability and time-dependent conversion of the A^* into the B phase as proposed by us earlier.[22]

In our experiments, we found that T_{A^*B} depends on the strength of the magnetic field (consistent with earlier work[3,34]) and is significantly suppressed compared to the zero-field results.[7,22] In Fig. 4 the solid triangles indicate the supercooled $A^* \rightarrow B$ transition and the open triangle shows the only $B \rightarrow A^*$ transition we observed on warming. For comparison, we plot the data of Gervais *et al.*[4] obtained at $P=25$ bar using a high-frequency transverse sound technique where solid circles denote the $A^* \rightarrow B$ transition and open circles the $B \rightarrow A^*$ transition. Our data show the hysteretic nature of the $A^* \rightarrow B$ transition and agree with the Northwestern group's results,[8,34] in contrast to the hybrid vibrating wire data of Brussaard *et al.*[3] where the $A^* \rightarrow B$ and $B \rightarrow A^*$ transitions occurred at almost the same temperature ($P=4.8$ and 7.4 bar).

The fact that our $B \rightarrow A^*$ transition was only seen at the highest field and was never observed at 1270 G (or 747 G) is very peculiar. According to the data of Gervais *et al.*[4] shown in Fig. 4 the $B \rightarrow A^*$ transition occurs approximately 230 μK higher than the $A^* \rightarrow B$ transition and the temperature offset only weakly depends on the field. If we use the same approach, namely, extrapolate the T_{BA^*} in our experiments by offsetting it by 400 μK (based on the 2130 G data), then we would predict T_{BA^*} at $B=1270$ G to occur at ≈ 1.6 mK. If the $B \rightarrow A^*$ transition temperature scales as B^2 (the limiting behavior in the $B \rightarrow 0$ limit), then the $B \rightarrow A^*$ transition should occur at ≈ 1.7 mK. These two temperatures form the boundaries of the gray box shown in Fig. 2B. Clearly, no signature of the $B \rightarrow A^*$ transition was observed at this temperature. We note that the results of Gervais *et al.*[4] also do not show a $B \rightarrow A^*$ transition below ~ 1400 G, even though they, too, should have adequate sensitivity to resolve this.

V. DISCUSSION

Figure 2 summarizes the ρ_s/ρ obtained in different fields and Fig. 2(D) shows the zero field values of ρ_s/ρ taken from.[22] In bulk ^{3}He-A, the superfluid density is a tensor quantity and is determined by the relative orientation of the orbital angular momentum vector $\mathbf{l}$ and the superflow.[32] To measure the anisotropic components of the superfluid density tensor it is necessary to orient the $\mathbf{l}$ texture of the superfluid. In the bulk, this can be achieved, for example, by taking advantage of the preferential orientation of the spins (perpendicular to the $\mathbf{d}$ vector) along the magnetic field direction, and the alignment of $\mathbf{d}$ with $\mathbf{l}$. The $\mathbf{l}$ texture is also oriented

perpendicular to the cell walls. With the field parallel to the walls, a uniform texture with $\rho_{s\perp}$ may be created with $\mathbf{l}$ perpendicular to the flow. By application of a magnetic field perpendicular to the walls, a nearly uniform texture may be created with $\mathbf{l}$ parallel to the wall, thus allowing $\rho_{s\|}$ to be inferred (the finite bending radius ~ 25 μm precludes a direct measurement of $\rho_{s\|}$ because of the nonuniform texture) and the ratio, $\rho_{s\perp}/\rho_{s\|}=2$, is only a limiting case. Torsional oscillator experiments[35] demonstrated the anisotropic nature of ρ_s/ρ in ^{3}He-A and also found consistency at 23 bar between the theoretically expected ratio of $\rho_{s\perp}/\rho_s^B=6/5$, as was later seen in experiments at Manchester.[36]

Aerogel is a medium that should be intrinsically isotropic. Presumably the superflow direction is highly local in orientation as the superfluid must bypass regions of high silica density (where superfluidity is most likely suppressed). Consequently, one would expect only a little anisotropy in $\rho_s^{A^*}/\rho$ to be revealed by the application of a magnetic field perpendicular to the axis of the cylindrical sample. It is possible that in zero field there might be local domains of the texture (possibly manifested by the broad NMR line shapes) and that a progressively larger field would orient these domains with $\mathbf{l}\|$ to the superflow. However, there is no evidence of any *decrease* in $\rho_s^{A^*}$ upon applying a field (compare the lower panel in Fig. 2 to the upper panel). We take this to imply that the superfluid density in the *A*-like phase is most likely isotropic.

If we assume the A^* phase to be the bulk *A* phase, then the results of two theoretical works[20,21] predict an anisotropy of the superfluid density tensor in aerogel. Higashitani's results[21] predict that the ratio of $\rho_{s\|}^A/\rho_{s\perp}^A \approx 0.5$ and that $\rho_s^B < \rho_{s\perp}^A$. Thus, the ratio of $\rho_{s\|}^A/\rho_s^B > 0.5$, in contrast to our experimental result, which shows a stronger suppression of $\rho_s^{A^*}$. Hänninen *et al.*[20] find the same expression for the superfluid density. However, they suggest that the suppression of $\rho_{s\|}^A$ should increase as the temperature is lowered, in contrast to the experimental observations. It is well known that the homogenous scattering models cannot account for the strong suppression of the superfluid density relative to T_c, and thus inhomogenous scattering models (reflecting local anisotropic scattering from the strand like aerogel) are thought to be more appropriate.[16,23] Despite the limitations of the homogenous scattering model, the size of the ratio $\rho_s^{A^*}/\rho_s^B \approx 0.5$, which is outside the bounds of the predictions of the theoretical work, together with the absence of any variation of ρ_s with magnetic field, suggest that the A^* phase cannot be unambiguously identified as the bulk ^{3}He *A*-phase. Indeed, recent theoretical works of Fomin[12,13] propose another equal-spin-paired state (axiplanar phase) as a stable *A*-like phase in the presence of disorder, though there are no accompanying predictions for the magnitude of the superfluid density in this phase.

In the bulk *B* phase in zero field, the energy gap Δ_B is isotropic and no anisotropy in the superfluid density is expected.[32] However, the presence of a magnetic field distorts Δ_B. Earlier ultrasound measurements in the bulk demonstrated the suppression of the energy gap by $\sim 8\%$ at $B=5$ kG and $P=29.3$ bar.[37,38] In our field range (up to 2.1 kG) the distortion is expected to be on the order of 1.5%, which implies a decrease of ρ_s^B/ρ by less than 1%, within the scatter of our measurements.

From the superfluid density shown in Fig. 2 and Eq. (3), we can deduce the zero-temperature energy gap for the *B* phase I,[33,39,40] which yields $\Delta_B \approx 0.5\Delta_{\text{bulk}}$, in agreement with the earlier NMR measurements of Barker *et al.*[5] and heat capacity data.[41]

In bulk ^{3}He the nucleation of the *B* phase from the *A* phase at the first-order transition can be explained in the framework of the free-energy and surface-energy differences between two phases.[42,43] This approach first assumes the nucleation of a seed of the *B* phase inside the metastable *A* phase. Once the size of a seed exceeds the critical radius R_c, the transition to the energetically favored *B* phase occurs rapidly. Experimentally, it has been shown that the *B* phase formation can be stimulated by radiation[42] and is also aided by any roughness at the bounding surfaces on a scale larger than the coherence length. The critical radius can be expressed as $R_c=2\sigma_{AB}/\Delta G$, where σ_{AB} is the surface tension between the two phases and ΔG is the bulk free-energy difference. Work of Osheroff and Cross[44] provided insight into the surface tension between the *A* and *B* phases in bulk ^{3}He and established that $\sigma_{AB} \sim F_s\xi(T)$. Here F_s is the difference between the normal phase and superfluid free energies at T_{AB} and the temperature-dependent coherence length, $\xi(T)$ is given by the expression

$$\xi(T) = [7\zeta(3)/48\pi^2]^{1/2}(\hbar v_F/k_B T_c)(1 - T/T_c)^{-1/2}$$
$$= 0.13(\hbar v_F/k_B T_c)(1 - T/T_c)^{-1/2}, \quad (4)$$

where $\zeta(3)$ is the Riemann Zeta function. We assume[45] that the free-energy difference $F_s \sim \Delta^2/\xi(T)^2$, take the values of T_c to be 2.41 mK in the bulk and 1.85 mK for ^{3}He in aerogel, and T_{AB} to be 1.95 mK in the bulk and 1.48 mK (at zero field) for ^{3}He in aerogel. We can then estimate the surface tension. Setting $\sigma_{AB}^{\text{aerogel}} \sim \Delta^2/\xi(T)$, from Eq. (4) we find that $\sigma_{AB}^{\text{aerogel}} \sim 0.19\sigma_{AB}^{\text{bulk}}$, comparable to the $0.25\sigma_{AB}^{\text{bulk}}$ reported by Gervais *et al.*[34] on a different aerogel sample near melting pressure.

The strong supercooling of the $A^* \rightarrow B$ transition in aerogel confirms that this is a first-order transition and the fact that its temperature is not affected by the cooling rate suggests that the temperature of the transition is determined mainly by the microstructure of aerogel, which strongly pins the A^*B interface. The Northwestern group's result for the critical radius of the seed of the *B* phase in the *A* phase is $R_c^{\text{aerogel}} \sim 5R_c^{\text{bulk}}$ (Ref. 34) and suggests a larger energy of the A^*-*B* interface. The $A^* \rightarrow B$ transition's finite width (~ 20 μK) also supports the argument that pinning dominates the dynamics of the interface. Our results for the transition's width are consistent with the earlier hybrid vibrating wire experiments by Brussaard *et al.*[3] and the recent experiments at Stanford.[9] We would also argue that in highly confined ^{3}He, such as that encountered in the experiments with large ^{4}He content,[46] pinning would likely ensure that only the A^* phase would be present.

In the bulk, it is generally acknowledged that even when the experiment is taken below the supercooled $A^* \rightarrow B$ transition, small seeds of the *A* phase remain trapped (perhaps in

corners of the cell), while the rest of the liquid is in the lower-energy B phase. When warming, the A phase regenerates without superheating from these seeds. Because we have a limited data set, we can only speculate that there is some critical field (in the region of 1400 G) above which the surface or pinning energy (that is a barrier to the propogation of the A^* phase) is overwhelmed by the difference in the free energies of the A^* and B phases. Certainly the critical radius is very large for disordered ^{3}He, and this fact together with pinning may explain why the A^* phase fails to reappear while warming in low fields. On the other hand, our only $B \rightarrow A^*$ transition was observed from a mixture of the A^* and B phases rather than the B phase alone, and this may have assisted to reestablish the A^* phase. Clearly there is a need for a thorough investigation of the hysteresis of the $A^* \rightarrow B$ transition in fields near 1400 G.

VI. CONCLUSION

We performed low-frequency sound measurements in ^{3}He confined in 98% aerogel in the presence of a magnetic field oriented perpendicular to the sound propogation direction. We observed the second sound like (slow) mode, and, from measurements of this mode's sound velocity versus temperature, we inferred the superfluid fraction ρ_s/ρ in both A^* and B phases. We did not observe any significant field dependence of ρ_s/ρ in either phase. However, $\rho_s^{A^*}/\rho$ and ρ_s^B/ρ differ in magnitude by a factor of two. This behavior is inconsistent with the evolution of the superfluid density in the bulk A phase and suggests that another equal spin-paired phase can be stable in the presence of disorder. We also argue that at a critical field around 1400 G, the free-energy difference between the two phases overcomes the pinning energy, enabling the transition from the B phase to the A^* phase.

ACKNOWLEDGMENT

The aerogel sample was grown by Norbert Mulders. We thank J. Baumgardner and D. Osheroff for sharing their results with us prior to publication and acknowledge useful discussions with I. Fomin, V. Dmitriev, and W. P. Halperin. Financial support was provided by the NSF(DMR-0071630,0202113) and by NATO SA(PST.CLG. 979379)6993/FP.

[1] J. V. Porto and J. M. Parpia, Phys. Rev. Lett. **74**, 4667 (1995).
[2] A. Golov, D. A. Geller, J. M. Parpia, and N. Mulders, Phys. Rev. Lett. **82**, 3492 (1999).
[3] P. Brussaard, S. N. Fisher, A. M. Guenault, A. J. Hale, N. Mulders, and G. R. Pickett, Phys. Rev. Lett. **86**, 4580 (2001).
[4] G. Gervais, T. M. Haard, R. Nomura, N. Mulders, and W. P. Halperin, Phys. Rev. Lett. **87**, 035701 (2001).
[5] B. I. Barker, Y. Lee, L. Polukhina, D. D. Osheroff, L. W. Hrubesh, and J. F. Poco, Phys. Rev. Lett. **85**, 2148 (2000).
[6] A. Golov, J. V. Porto, and J. M. Parpia, Phys. Rev. Lett. **80**, 4486 (1998).
[7] E. Nazaretski, N. Mulders, and J. M. Parpia, J. Low Temp. Phys. **134**, 763 (2004).
[8] G. Gervais, K. Yawata, N. Mulders, and W. P. Halperin, Phys. Rev. B **66**, 054528 (2002).
[9] J. E. Baumgardner, Y. Lee, D. D. Osheroff, L. W. Hrubesh, and J. F. Poco, Phys. Rev. Lett. **93** 055301 (2004).
[10] C. L. Vicente, H. C. Choi, J. S. Xia, W. P. Halperin, N. Mulders, and Y. Lee (unpublished).
[11] V. V. Dmitriev, I. V. Kosarev, N. Mulders, V. V. Zavjalov, and D. Ye. Zmeev, Physica B **329–333**, 320 (2003).
[12] I. A. Fomin, Pis'ma Zh. Eksp. Teor. Fiz. **77**, 285 (2003) [JETP Lett. **77**, 240 (2003)].
[13] I. A. Fomin, J. Low Temp. Phys. **134**, 769 (2004).
[14] J. Baumgardner and D. D. Osheroff (unpublished).
[15] E. V. Thuneberg, S.-K. Yip, M. Fogelström, and J. A. Sauls, Phys. Rev. Lett. **80**, 2861 (1998).
[16] R. Hänninen and E. V. Thuneberg, Phys. Rev. B **67**, 214507 (2003).
[17] P. Sharma and J. A. Sauls, J. Low Temp. Phys. **125**, 115 (2001).
[18] H. Alles, J. J. Kaplinsky, P. S. Wootton, J. D. Reppy, J. H. Naish, and J. R. Hook, Phys. Rev. Lett. **83**, 1367 (1999).
[19] V. V. Dmitriev, V. V. Zavjalov, D. E. Zmeev, I. V. Kosarev, and N. Mulders, Pis'ma Zh. Eksp. Teor. Fiz. **79**, 612 (2003); JETP Lett. **76**, 312 (2002).
[20] R. Hänninen, T. Setälä, and E. V. Thuneberg, Physica B **255**, 11 (1998).
[21] S. Higashitani, J. Low Temp. Phys. **114**, 161 (1999).
[22] E. Nazaretski, N. Mulders, and J. M. Parpia, Pis'ma Zh. Eksp. Teor. Fiz. **79**, 470 (2004) [JETP Lett. **79**, 383 (2004)].
[23] J. A. Sauls and Priya Sharma, Phys. Rev. B **68**, 224502 (2003).
[24] H. C. Choi, A. J. Gray, C. L. Vicente, J. S. Xia, G. Gervais, W. P. Halperin, N. Mulders, and Y. Lee, Phys. Rev. Lett. **93**, 145302 (2004).
[25] G. Barton and M. A. Moore, J. Phys. C **7**, 4220 (1974).
[26] Y. H. Li and T. L. Ho, Phys. Rev. B **38**, 2362 (1988).
[27] A. B. Vorontsov and J. A. Sauls, Phys. Rev. B **68**, 064508 (2003).
[28] L. D. Landau, J. Phys. (USSR) **5**, 71 (1941).
[29] M. J. McKenna, T. Slawecki, and J. D. Maynard, Phys. Rev. Lett. **66**, 1878 (1991).
[30] E. Nazaretski, G. Lawes, D. M. Lee, N. Mulders, D. Ponarin, and J. M. Parpia, J. Low Temp. Phys. **126**, 685 (2002).
[31] N. Mulders, R. Mehrotra, Lori S. Goldner, and G. Ahlers, Phys. Rev. Lett. **67**, 695 (1991).
[32] A. J. Leggett, Rev. Mod. Phys. **47**, 331 (1975).
[33] J. M. Parpia, D. G. Wildes, J. Saunders, E. K. Zeise, J. D. Reppy, and R. C. Richardson, J. Low Temp. Phys. **61**, 337 (1985).
[34] G. Gervais, K. Yawata, N. Mulders, and W. P. Halperin, Phys. Rev. Lett. **88**, 045505 (2002).
[35] J. E. Berthold, R. W. Giannetta, E. N. Smith, and J. D. Reppy, Phys. Rev. Lett. **37**, 1138 (1976).
[36] J. R. Hook, E. Faraj, S. G. Gould, and H. E. Hall, J. Low Temp. Phys. **74**, 45 (1989).
[37] R. Movshovich and D. M. Lee, J. Low Temp. Phys. **89**, 515 (1992).
[38] R. Movshovich, N. Kim, and D. M. Lee, Phys. Rev. Lett. **64**, 431

(1990).
[39] G. Lawes and J. M. Parpia, Phys. Rev. B **65**, 092511 (2002).
[40] Dietrich Einzel, J. Low Temp. Phys. **54**, 427 (1984).
[41] Jizhong He, A. D. Corwin, J. M. Parpia, and J. D. Reppy, Phys. Rev. Lett. **89**, 115301 (2002).
[42] P. Schiffer, D. D. Osheroff, and A. J. Leggett, in *Progress in Low Temperature Physics*, edited by W. P. Halperin (Elsevier, Amsterdam, 1995), Vol. XIV, p. 159.
[43] A. J. Leggett, Phys. Rev. Lett. **53**, 1096 (1984).
[44] D. D. Osheroff and M. C. Cross, Phys. Rev. Lett. **38**, 905 (1977).
[45] A. J. Leggett and S. K. Yip, in *Superfluid ^{3}He*, edited by L. P. Pitaevskii and W. P. Halperin (Elsevier, Amsterdam, 1990), p. 523.
[46] G. Lawes, A. I. Golov, E. Nazaretski, N. Mulders, and J. M. Parpia, Phys. Rev. Lett. **90** 195301 (2003).